Article

Discovery Medicine 2024; 36(189): 2088–2097
https://doi.org/10.24976/Discov.Med.202436189.193

Propofol Ameliorates Sepsis-Induced Myocardial Dysfunction via Anti-Apoptotic, Anti-Oxidative Properties, and mTOR Signaling

Lijun Xie[1], Meiling Zhao[2], Liwu Zong[1], Yifeng Yue[1,*]

[1]Department of Anesthesiology, Zibo Central Hospital, 255000 Zibo, Shandong, China
[2]Department of Critical Care Medicine, Zibo Central Hospital, 255000 Zibo, Shandong, China
*Correspondence: yueyifeng1982@163.com (Yifeng Yue)
Published: 20 October 2024

Background: Sepsis often leads to cardiomyopathy, contributing to increased mortality rates. 2,6-Diisopropylphenol (propofol), an anesthetic, has demonstrated efficacy in protecting cardiomyocytes from cell death caused by hypoxia and reoxygenation. This study examined the effects of propofol on sepsis-associated myocardial dysfunction and explored the underlying mechanism of action.

Methods: Mice and rat cardiomyocytes (H9C2 cell line) were used to establish a sepsis-induced myocardial dysfunction model. Lipopolysaccharides (LPS)-treated mice and H9C2 cells were treated with propofol, with rapamycin used for mechanistic studies in H9C2 cells. Cardiac function was evaluated by echocardiographic measurements. Heart tissues were stained with hematoxylin and eosin, and heart weight/body weight ratio along with the levels of cardiac biomarkers were measured using Enzyme Linked Immunosorbent Assay (ELISA). Activation of the mammalian target of rapamycin (mTOR) pathway was assessed by western blotting. Apoptosis in heart tissues and H9C2 cells was evaluated using Terminal deoxynucleotidyl transferase (TdT) dUTP nick end labeling (TUNEL) assay, and cell viability was quantified using Cell Counting Kit (CCK)-8 assay. Oxidative stress in H9C2 cells was assessed by measuring reactive oxygen species (ROS) levels through immunofluorescence staining and malondialdehyde (MDA) and superoxide dismutase (SOD) levels using ELISA.

Results: Propofol reversed LPS-induced myocardial changes and cardiac dysfunction ($p < 0.05$). In mouse tissues and H9C2 cells, propofol reversed LPS-induced mTOR pathway inhibition and apoptosis ($p < 0.001$). Moreover, propofol alleviated oxidative stress in LPS-treated cells. The activation of the mTOR pathway by propofol, along with its inhibitory effects on oxidative stress and apoptosis in cardiomyocytes, was negated by rapamycin ($p < 0.001$).

Conclusion: Propofol ameliorates sepsis-induced myocardial dysfunction triggered by LPS through the mTOR pathway, thereby promoting antioxidative stress and reducing cell apoptosis.

Keywords: sepsis; myocardial dysfunction; propofol; mTOR; cardiomyocyte

Introduction

Sepsis, a life-threatening dysfunction of organs resulting from a dysregulated host response, is a major cause of mortality [1]. Cardiomyopathy, characterized by decreased left ventricular (LV) contractility, is common during sepsis and is associated with mitochondrial dysfunction, oxidative stress, inflammation, and cell death [2,3]. Sepsis-induced cardiomyopathy is a leading cause of death, despite efforts to prevent and manage the condition [4]. Therefore, an understanding of its underlying mechanisms is crucial for the development of safe and effective treatments.

2,6-Diisopropylphenol (propofol) is widely used as an anesthetic for its sedative and general-anesthesia properties [5]. Propofol offers many advantages in clinical settings, including ideal pharmacokinetic and pharmacodynamic profiles, along with quick induction and recovery times, minimal residual effects, and lack of respiratory irritation [6]. Besides its anesthetic effects, propofol mitigates myocardial ischemic reperfusion injury [7,8], inhibits tumor growth and metastasis [9–12], and protects against cardiomyocyte injury induced by hypoxia and reoxygenation as well as lipopolysaccharides (LPS) [13,14]. It also mitigates acute kidney injury induced by sepsis [15]. Therefore, propofol may provide protective benefits to patients with sepsis, reducing myocardial injury and dysfunction. However, its precise impact on sepsis-induced myocardial dysfunction is not fully understood.

In the present study, we used mice and H9C2 cells and treated them with LPS to induce myocardial dysfunction. We investigated the impact of propofol in mitigating septic-induced cardiomyopathy and further explored the underlying mechanisms.

Materials and Methods

Animal Treatments

All experimental procedures complied with ethical standards for the care and use of animals and were approved by the Ethics Committee of Zibo Central Hospital (Approval No. 2024054). Thirty C57BL/6J mice (male, 22 ± 2 g; age, 8 weeks) were obtained from Beijing Vital River Laboratory Animal Technology Co., Ltd. (Beijing, China) and given food and water. Mice were housed in a specific-pathogen-free environment, with a temperature of 24 ± 2 °C, a humidity of 50–60%, and 12-hour light/dark cycles. Mice were randomly divided into three groups: (1) Control; (2) Model, myocardial dysfunction was induced by sepsis through intraperitoneal injections of 10 mg/kg LPS (BS904, Biosharp Life Science, Hefei, Anhui, China) [16]; and (3) Model+propofol, mice were intraperitoneally injected with 50 mg/kg propofol (MedChemExpress) 2 h before being treated with LPS (10 mg/kg) as described above [15]. Each group consisted of ten mice (n = 10). Cardiac function was evaluated 12 h post-treatment, followed by euthanasia (50% CO_2) to collect serum and heart tissues. The efficacy of the myocardial dysfunction model was confirmed through echocardiographic assessments. The myocardial dysfunction model proved to be effective, with no animals excluded from the analysis.

Echocardiography and Sample Collection

At 24 h post-LPS injection, the mice were mildly sedated using 3% isoflurane and subjected to echocardiographic assessments, which were performed using the Vevo 3100 instrument (VisualSonics Inc., Tokyo, Japan). Next, mice were euthanized, body weight and heart weight were obtained, and heart tissues were collected and stored at –80 °C for subsequent assays.

Hematoxylin and Eosin Staining

Heart tissues were retrieved from –80 °C and fixed in 4% paraformaldehyde (P0099, Beyotime, Shanghai, China) for 2 h. Next, the tissues were embedded in paraffin and cut into 4-µm thick sections, followed by staining with hematoxylin for 10 min and eosin (C0105, Beyotime, Shanghai, China) for 3 min. The stained sections were examined under a CK31 light microscope (CKX31, Olympus, Tokyo, Japan).

Cell Treatments

Rat cardiomyocytes (H9C2 cell line, iCell-r012, iCell Bioscience Inc., Shanghai, China) were cultured in Dulbecco's Modified Eagle Medium (DMEM) (iCell-0001, iCell Bioscience Inc., Shanghai, China) supplemented with 10% fetal bovine serum (FBS; C0226, Beyotime, Shanghai, China) and penicillin-streptomycin (iCell-15140-122, iCell Bioscience, Inc.) and incubated at 37 °C in a 5% CO_2 environment. Cell authenticity was ensured by short tandem repeat profiling, and mycoplasma tests were performed. Cells were divided into 4 groups as follows: (1) NC, where cells were cultured normally with no treatments as the negative control; (2) LPS, where cells were treated with 10 µg/mL LPS for 12 h to establish a model of cardiac cell injury [16]; (3) LPS+propofol, where cells were treated with 50 µM propofol (24 h) and then with 12-h of 10 µg/mL LPS [14]; and (4) LPS+propofol+rapamycin and LPS+propofol, where cells were treated with 50 µM propofol and 10 nM rapamycin (HY-10219, MedChemExpress, Monmouth Junction, NJ, USA) for 24 h and then with 12 h of 10 µg/mL LPS [17].

Enzyme Linked Immunosorbent Assay (ELISA)

Heart tissue samples were processed with a homogenizer (CN-41056-98, Cole-Parmer Instrument Company, LLC., Shanghai, China) using lysis buffer (P0013, Beyotime, Shanghai, China). Levels of cardiac troponin-I (cTnI; SEKR-0048, Solarbio, Beijing, China), cardiac troponin-T (cTnT; SEKR-0047, Solarbio, Beijing, China), and creatine kinase MB (CK-MB; ab285231, Abcam, Cambridge, MA, USA) were measured using Enzyme Linked Immunosorbent Assay (ELISA) Kits (ab285231, Abcam, Cambridge, MA, USA). The cells were centrifuged at 1000 g for 10 min, and the concentrations of superoxide dismutase (SOD; A001-1, Jiancheng, Nanjing, China) and malondialdehyde (MDA; A003-1, Jiancheng, Nanjing, China) were measured. The optical density (OD value) was recorded at 450 nm using a Varioskan Lux microplate reader (VL0000D0, Thermo Fisher Scientific, Shanghai, China).

Western Blotting

Proteins were extracted using radioimmunoprecipitation assay buffer (P0013, Beyotime, Shanghai, China) supplemented with protease inhibitors (ST2573, Beyotime, Shanghai, China). Protein concentration was quantified using a protein assay kit (P0010S, Beyotime, Shanghai, China), and proteins were separated by 10% sodium dodecyl sulfate-polyacrylamide gel electrophoresis (SDS-PAGE; P0012A, Beyotime, Shanghai, China). After transferring proteins to polyvinylidene difluoride membranes (IPVH00010, Millipore, Billerica, MA, USA), they were blocked with 5% nonfat milk at room temperature for 15 min, and membranes were incubated overnight at 4 °C with primary antibodies for glyceraldehyde-3-phosphate dehydrogenase (GAPDH) (1:1000 dilution; TA-08, ZSGB Biotechnology, Beijing, China), mammalian target of rapamycin (mTOR) (1:1000 dilution; ab32028, Abcam, Cambridge, MA, USA), phosphorylated mTOR (p-mTOR) (ab109268, Abcam, Cambridge, MA, USA), B-cell lymphoma 2 (Bcl-2) (1:1000 dilution; ab182858, Abcam, Cambridge, MA, USA), and cleaved caspase-3 (1:1000 dilution; ab2302, Abcam, Cambridge, MA, USA). This was followed by a 2-h room temperature incubation with horseradish peroxidase-linked anti-rabbit secondary

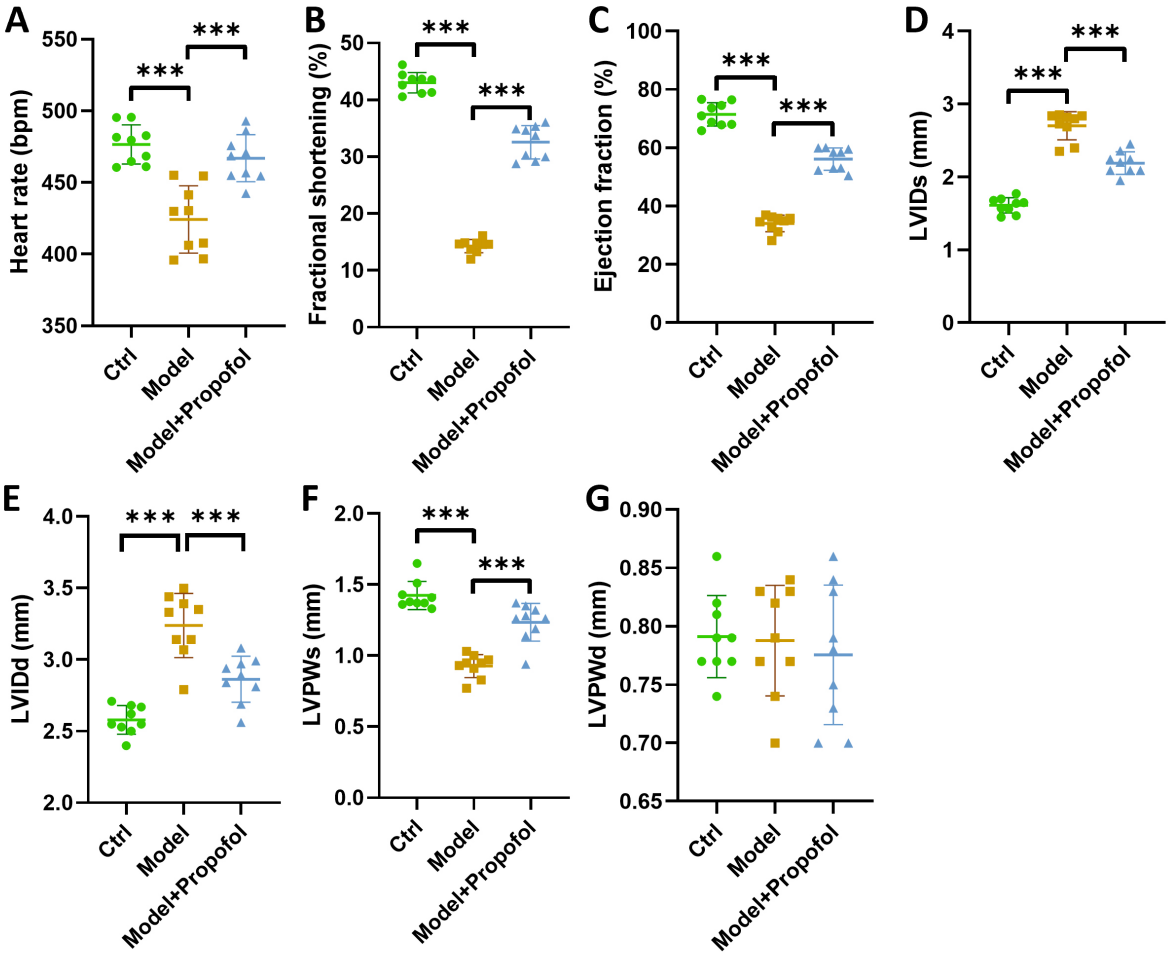

Fig. 1. 2,6-Diisopropylphenol (propofol) enhances cardiac function in a mouse model of sepsis-induced myocardial dysfunction. (A–G) Heart rate (A), fractional shortening (B), ejection fraction (C), left ventricular internal dimension systole (LVIDs, D), left ventricular internal dimension diastole (LVIDd, E), left ventricular internal dimension diastole (LVPWs, F), and left ventricular posterior wall systolic dimension (LVPWd, G) of mice models. N = 10. ***$p < 0.001$. Control values were used as a baseline to normalize the treatment group values. Ctrl, Control.

antibody (1:2000, ZB-2305, ZSGB Biotechnology, Beijing, China) and detection chemiluminescence with the enhanced chemiluminescence (ECL; 34075, Thermo Scientific, Shanghai, China) detection reagents. Grayscale analysis was conducted using ImageJ version 1.48 software (National Institutes of Health, Bethesda, MD, USA).

Reactive Oxygen Species (ROS) Detection

Cells were plated in 6-well plates at 5×10^6 cells/mL and grown under specified conditions. To measure the reactive oxygen species (ROS) levels, cells were treated with 2-7′ dichlorodihydrofluorescein diacetate (DCFH-DA; S0033S, Beyotime, Shanghai, China) for 20 min in darkness and then stained with 2-(4-amidinophenyl)-6-indolecarbamidine dihydrochloride (DAPI; C1002, Beyotime, Shanghai, China) at room temperature for 15 min. The fluorescence signal from DCFH-DA was used to assess the ROS levels, which were visualized with a CKX53 fluorescent microscope (OLYMPUS, Tokyo, Japan) and analyzed using ImageJ software (version 1.48, NIH, Rockville, MD, USA).

Cell Counting Kit (CCK)-8 Assay

Cells were seeded into 96-well plates at a concentration of 2×10^3 cells/mL. After 24 h of incubation, 10 µL of CCK-8 solution (G4103-5ML, Servicebio, Wuhan, China) was added to each well, and after an additional 2 h, the absorbance at 450 nm was measured using a DR-200Bs microplate reader (Diatek, Jiangsu, China).

Terminal Deoxynucleotidyl Transferase (TdT) dUTP Nick End Labeling (TUNEL)

Cells were grown in 12-well plates, fixed for 30 min with 4% paraformaldehyde, and permeabilized with 0.3% Triton X-100 (P0096, Beyotime, Shanghai, China) for 5

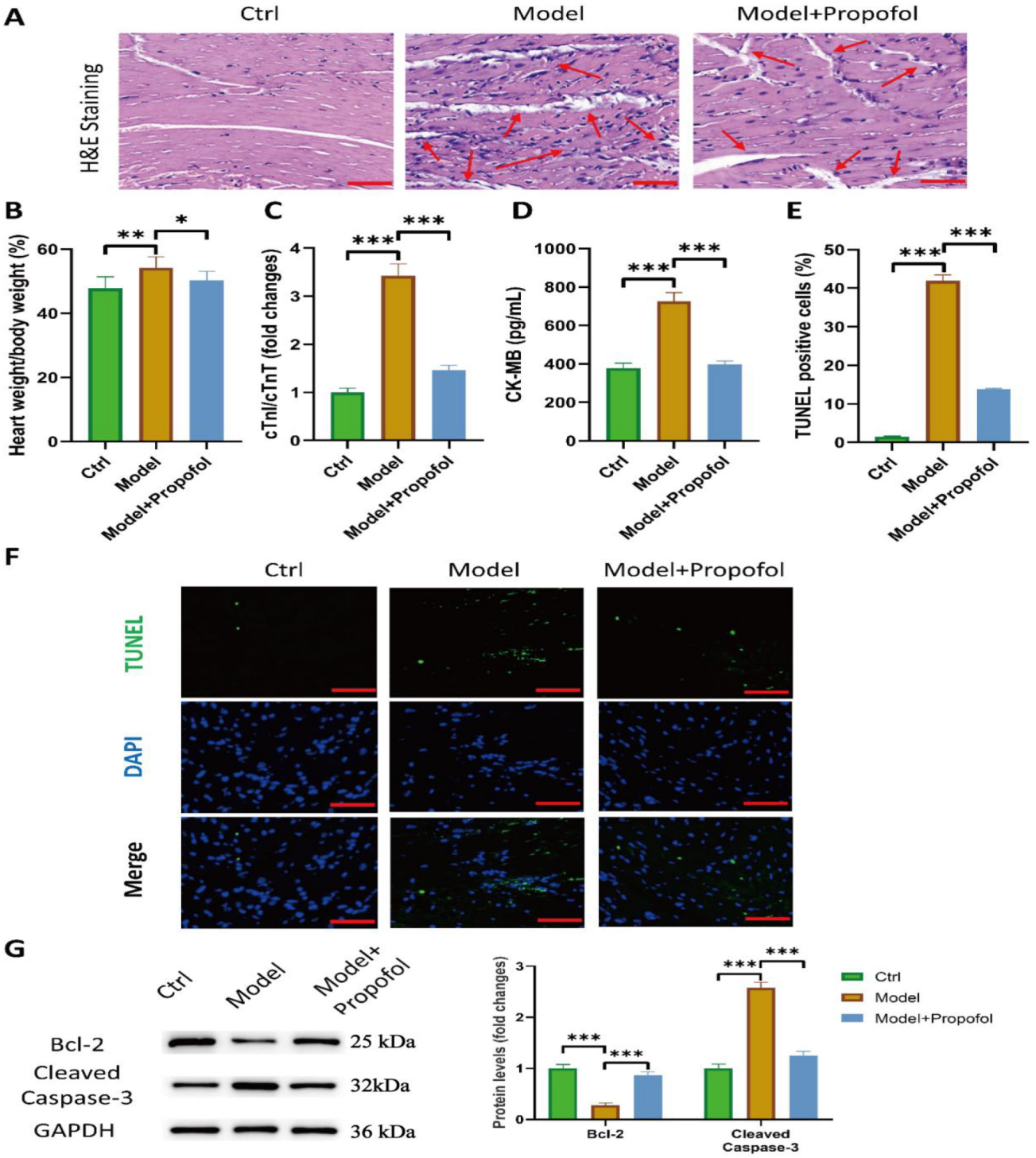

Fig. 2. Propofol mitigates myocardial injury and reduces apoptosis in heart tissues from mice with sepsis-induced myocardial dysfunction. (A) Hematoxylin and eosin staining (H&E staining) of heart tissues from mice (scale bar: 50 µm; red arrows indicate histological injury). (B) Heart weight/body weight ratio. (C) Ratio of cardiac troponin-I (cTnI)/cardiac troponin-T (cTnT) in heart tissue extract. (D) Creatine kinase MB (CM-KB) level in heart tissue extract. (E,F) Terminal deoxynucleotidyl transferase (TdT) dUTP nick end labeling (TUNEL) staining of heart tissues from mice (scale bar: 100 µm). Some DNA was degraded upon myocardial injury, leading to 2-(4-amidinophenyl)-6-indolecarbamidine dihydrochloride (DAPI) staining. (G) Levels of cleaved caspase 3 and B-cell lymphoma 2 (Bcl-2) protein, as detected by western blotting. N = 10. *$p < 0.05$, **$p < 0.01$, ***$p < 0.001$. Control values were used as a baseline to normalize the treatment group values. GAPDH, glyceraldehyde-3-phosphate dehydrogenase.

min. Similarly, heart tissue sections (4-µm thick) were fixed in 4% paraformaldehyde for 2 h and then permeabilized using proteinase K (P9460, Solarbio, Beijing, China) for 20 min. Next, Terminal deoxynucleotidyl transferase (TdT) dUTP nick end labeling (TUNEL) kits (40306ES60, Yeasen, Shanghai, China) of C1090 or C1088 (either red or green fluorescence) were used to stain cells or tissues, respectively, according to the manufacturer's instructions. Cells and tissue sections were observed using a CKX53 fluorescence microscope (OLYMPUS, Tokyo, Japan) at 450–550 nm. Apoptotic cells in four random fields of view were counted, and the cell apoptosis rate was determined as a ratio of the TUNEL-labeled cell number to the DAPI-labeled cell number.

Statistical Analyses

Data were expressed as mean ± standard deviation. Before comparing groups, the normality of all datasets was assessed using the Shapiro-Wilk test. Upon establishing a normal distribution, group comparisons were conducted using one-way analysis of variance with Tukey's post hoc test for multiple comparisons. All statistical evaluations were carried out using GraphPad Prism version 8.0.2 software (GraphPad Software, La Jolla, CA, USA), and a p-value less than 0.05 was deemed statistically significant.

Results

Propofol Improves the Cardiac Function in Mice with Sepsis-Induced Myocardial Dysfunction

Echocardiography results revealed significant changes in heart function between LPS-treated mice (model group) and controls. Specifically, heart rate (Fig. 1A), fractional shortening (Fig. 1B), ejection fraction (Fig. 1C), and left ventricular posterior wall diastolic dimension (LVPDs, Fig. 1F) were significantly reduced ($p < 0.001$). Conversely, left ventricular internal dimension systole (LVIDs, Fig. 1D) was significantly increased ($p < 0.001$). Left ventricular internal dimension diastole (LVIDd, Fig. 1E) decreased significantly after Propofol treatment ($p < 0.001$). Left ventricular post-systolic diameter (LVPWd, Fig. 1G) did not differ significantly between treatments. These results indicate the sepsis-induced myocardial dysfunction model was successfully established. Moreover, propofol reversed the echocardiography results, indicating propofol ameliorates cardiac dysfunction in the LPS mouse model.

Propofol Mitigates Myocardial Injury and Reduces Apoptosis in Heart Tissues from Mice with Sepsis-Induced Myocardial Dysfunction

Hematoxylin and eosin staining results (Fig. 2A) showed histological alterations in heart tissues of LPS-treated mice, including ruptured myocardial fibers and interstitial edema. However, these changes were mitigated by propofol treatment. The heart weight/body weight ratio (Fig. 2B), cTnI/cTnT ratio (Fig. 2C) and CK-MB level (Fig. 2D) were increased in model mice by subsequently decreased after administration of propofol ($p < 0.05$). These results demonstrate the efficacy of propofol in alleviating sepsis-induced myocardial dysfunction. Moreover, the percentage of TUNEL-positive cells (Fig. 2E,F) and the level of cleaved caspase-3 protein (Fig. 2G) increased, while the Bcl-2 protein level (Fig. 2G) decreased in the model mice, and these changes were reversed by propofol ($p < 0.001$), indicating propofol inhibits apoptosis in the heart of model mice.

Propofol Restores mTOR Pathway Inhibition in Heart Tissues of Mice with Sepsis-Induced Myocardial Dysfunction

In heart tissues (Fig. 3A), the ratio of phosphorylated mTOR to total mTOR (p-mTOR/mTOR) was reduced in the Model group compared to the Control group, and this effect was reversed by propofol ($p < 0.001$). Moreover, the p-mTOR/mTOR ratio was decreased in LPS-treated cardiomyocytes, but propofol treatment increased it (Fig. 3B). The enhancing effect of propofol was disrupted by the mTOR selective inhibitor rapamycin ($p < 0.001$), revealing the mTOR pathway was suppressed in LPS-induced models, while propofol promoted the mTOR pathway. In the propofol-treated cell model, rapamycin also inhibited mTOR signaling.

Propofol Increases Cardiomyocyte Viability and Protects Them from LPS-Induced Apoptosis by Activating the mTOR Pathway

Cell viability (Fig. 4A) was decreased by LPS treatment ($p < 0.001$) but propofol reversed it ($p < 0001$). However, mTOR pathway inhibition by the addition of rapamycin suppressed cell viability ($p < 0.001$).

Fig. 4B–D demonstrate that propofol reversed the decrease in Bcl-2 and the increase in cleaved caspase-3 in LPS-treated H9C2 cells. However, these effects were not observed when the mTOR inhibitor rapamycin was used ($p < 0.001$). These results indicate that propofol protected H9C2 cells against LPS-induced apoptosis when the mTOR pathway is not inhibited, consistent with the results of the TUNEL assay (Fig. 4E,F), demonstrating that propofol mitigates the increased apoptosis rate even without the addition of rapamycin ($p < 0.001$).

Propofol Safeguards Cardiomyocytes from LPS-Induced Oxidative Stress by Activating the mTOR Pathway

Fig. 5A,B shows that the ROS level (represented by the fluorescent intensity of DCFH-DA) was increased in LPS-treated H9C2 cells, and this change was reversed by propofol, while the reversal of the ROS level was disrupted by rapamycin ($p < 0.001$). Moreover, propofol reversed

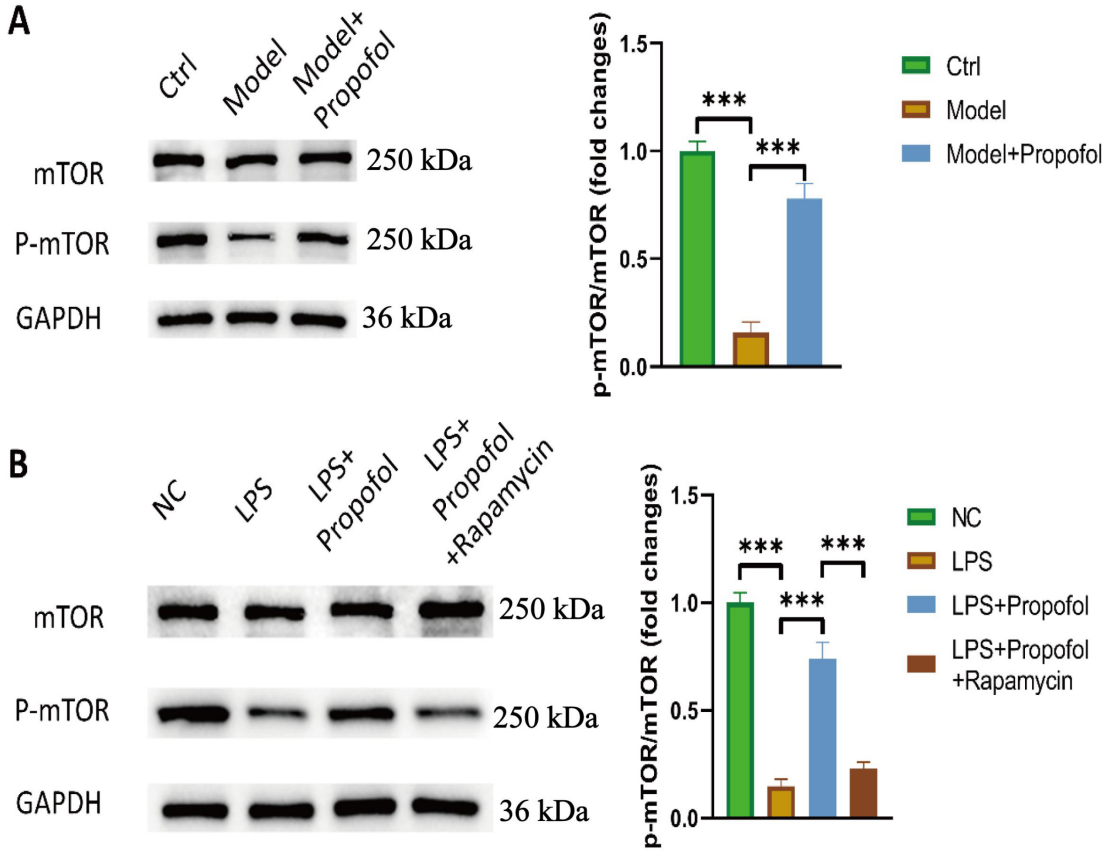

Fig. 3. Propofol restores mammalian target of rapamycin (mTOR) pathway inhibition in heart tissues of mice with sepsis-induced myocardial dysfunction. (A,B) Levels of mTOR and phosphorylated mTOR (p-mTOR) protein in mice heart tissues (A, N = 10) and cardiomyocytes (H9C2) (B, N = 5), as detected by western blotting. ***$p < 0.001$. Control values were used as baseline to normalize the treatment group values. NC, negative control; LPS, lipopolysaccharides.

the increased MDA level (Fig. 5C) and the decreased SOD level (Fig. 5D) in LPS-treated H9C2 cells, while the reversing effect of propofol was disrupted by rapamycin ($p < 0.001$). These findings indicate that propofol protects H9C2 cells from LPS-induced oxidative stress, provided that the mTOR pathway is not inhibited.

Discussion

This study demonstrated that propofol effectively improves myocardial function and mitigates damage and apoptosis in cardiomyocytes affected by LPS-induced cardiomyopathy. Furthermore, propofol reduces ROS production and apoptosis in LPS-treated H9C2 cells by activating the mTOR pathway.

Sepsis is a syndrome of physiological, pathological, and biochemical abnormalities triggered by the body's response to infection [18–20]. In severe cases, septic shock is characterized by significant circulatory and cellular dysfunction, greatly increasing the risk of death [20]. One common manifestation of sepsis is myocardial depression or cardiac dysfunction [21], which are characterized by reduced myocardial contraction and ejection fraction, which can elevate mortality rates [19,21]. However, the precise molecular mechanisms underlying sepsis-induced myocardial depression remain incompletely understood.

In our study, we established a model of myocardial dysfunction induced by sepsis and observed that propofol significantly improved myocardial dysfunction caused by LPS. This finding is consistent with the research of Han *et al.* [22], which showed that propofol can alleviate myocardial dysfunction in mice with endotoxemia. Cardiomyocyte apoptosis is recognized as a primary factor contributing to cardiac dysfunction in patients with sepsis [23,24], and our study revealed that propofol inhibits apoptosis in mice with sepsis-induced myocardial dysfunction. Similarly, Tang *et al.* [25] demonstrated propofol's efficacy in alleviating myocardial dysfunction in mice with endotoxemia, suggesting propofol mitigates sepsis-induced cardiac dysfunction by inhibiting apoptosis.

In our investigation into how propofol mitigates sepsis-induced cardiac dysfunction by inhibiting apoptosis, we discovered a crucial role for the mTOR pathway in this process. An earlier study indicated that alterations in myocardial mTOR signaling may contribute to myocardial dysfunction [26]. mTOR is essential in the preven-

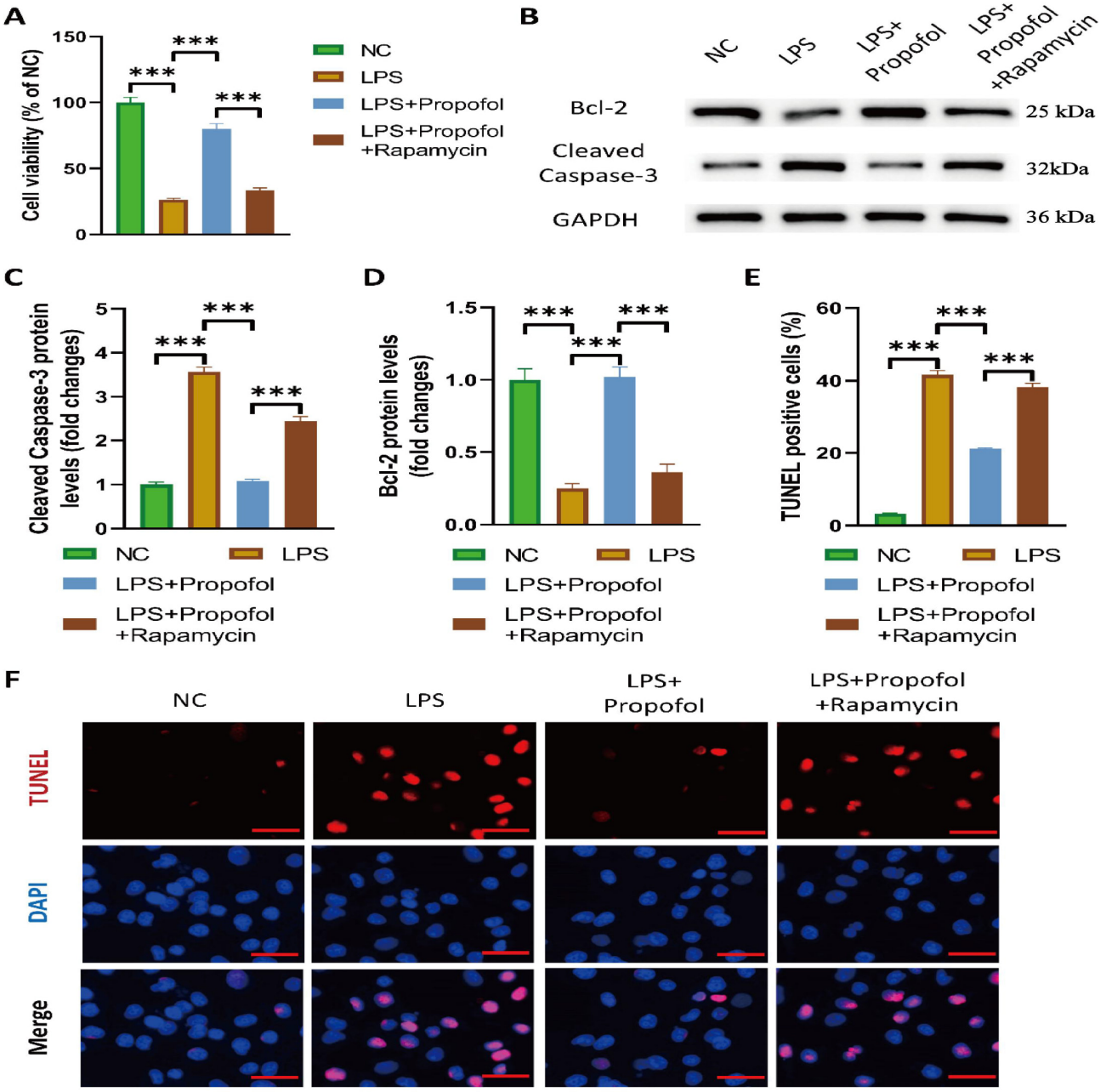

Fig. 4. Propofol increases cardiomyocyte viability and protects them from LPS-induced apoptosis by activating the mTOR pathway. (A) Cell viability detected by Cell Counting Kit-8 assay. (B–D) Levels of cleaved caspase-3 and Bcl-2 protein in cardiomyocytes (H9C2) as detected by western blotting (E,F). TUNEL staining results for cardiomyocytes cells H9C2 (scale bar: 50 µm). N = 5. ***$p < 0.001$, Control values were used as a baseline to normalize the treatment group values.

tion of cardiac hypertrophy and cardiac dysfunction in animal models [27]. Our findings showed that inhibiting mTOR significantly reduced the cardioprotective effects of propofol on sepsis-induced cardiac dysfunction. Additional research revealed that inhibiting mTOR exacerbates propofol-induced apoptosis [25]. Wang *et al.* [27] reported that activated AMPK (AMP-activated protein kinase), which downregulates mTOR expression, thereby improving cardiac dysfunction following myocardial infarction. Conversely, Zhang *et al.* [28] demonstrated that inhibiting mTOR promoted apoptosis and exacerbated cardiac dysfunction. Discrepancies in these results can be attributed to several factors, including differences in models, dosage and timing of rapamycin administration, and cell type-specific effects. Moreover, one study has shown that ROS, and reactive nitrogen species destroy mitochondrial membranes and trigger apoptosis in the heart, creating a vicious cycle of ROS generation that intensifies myocardial injury and dysfunction [29]. Our research demonstrated that propofol protects H9C2 cells from LPS-induced

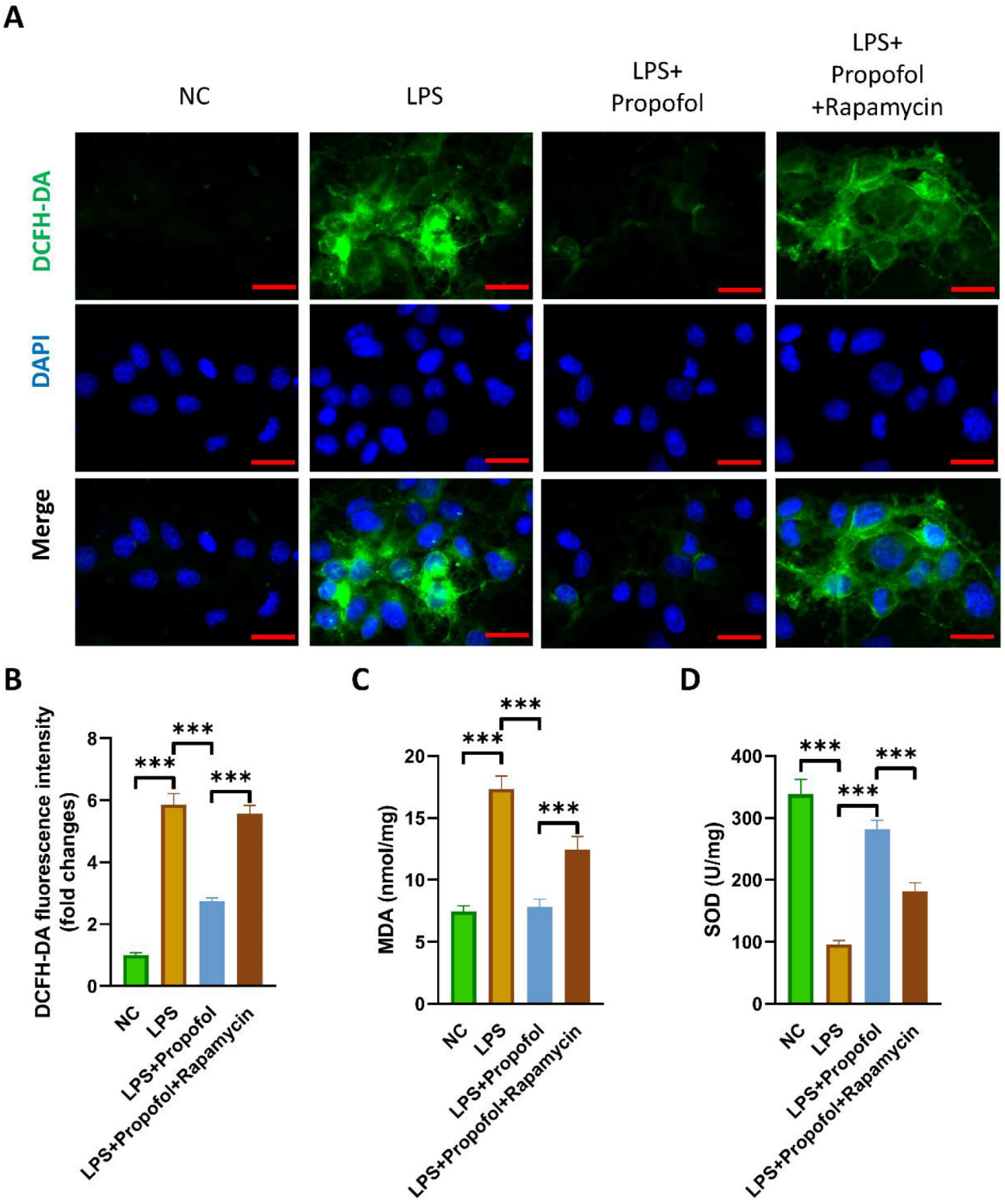

Fig. 5. Propofol safeguards cardiomyocytes from LPS-induced oxidative stress by activating the mTOR pathway. (A,B) Reactive oxygen species (ROS) in cardiomyocytes as detected by immunofluorescence (scale bar: 50 μm). (C,D) Levels of malondialdehyde (MDA) and superoxide dismutase (SOD) in cardiomyocytes (H9C2) measured by Enzyme Linked Immunosorbent Assay (ELISA). N = 5. ***$p < 0.001$. Control values were used as a baseline to normalize the treatment group values. DCFH-DA, 2-7′ dichlorodihydrofluorescein diacetate.

oxidative stress, while mTOR pathway inhibition exacerbates ROS production, further worsening myocardial injury and dysfunction. These findings align with those of other studies [25,30,31], suggesting propofol alleviates sepsis-induced myocardial injury and dysfunction by inhibiting ROS production through the mTOR pathway.

Conclusion

In conclusion, this study demonstrated that propofol protects against LPS-induced cardiac dysfunction by activating the mTOR pathway. Moreover, propofol attenuates oxidative stress and apoptosis, suggesting its potential as a therapy for sepsis-induced myocardiopathy. However, limitations, such as reliance on animal models that may not fully replicate human physiological responses, exist. Future research should validate these findings in clinical trials to assess its safety and efficacy in patients with sepsis-induced cardiac dysfunction. Additionally, in-depth investigations are necessary to decode the intricate molecular mechanisms by which propofol influences mTOR signaling and to explore its potential synergistic effects with other pharmacological interventions.

Availability of Data and Materials

The corresponding author will provide the data that underpin the study's conclusions with a reasonable application.

Author Contributions

LJX and YFY designed the study; LJX, MLZ, LWZ, and YFY conducted the study; MLZ collected and analyzed the data; LWZ participated in drafting the manuscript. All authors contributed to critical revision of the manuscript for important intellectual content. All authors gave final approval of the version to be published. All authors participated fully in the work, took public responsibility for appropriate portions of the content, and agreed to be accountable for all aspects of the work in ensuring that questions related to the accuracy or completeness of any part of the work are appropriately investigated and resolved.

Ethics Approval and Consent to Participate

All experimental procedures complied with ethical standards for the care and use of animals and were approved by the Ethics Committee of Zibo Central Hospital (Approval No. 2024054).

Acknowledgment

Not applicable.

Funding

This research received no external funding.

Conflict of Interest

The authors declare no conflict of interest.

References

[1] Srzić I, Nesek Adam V, Tunjić Pejak D. Sepsis definition: what's new in the treatment guidelines. Acta Clinica Croatica. 2022; 61: 67–72.

[2] Carbone F, Liberale L, Preda A, Schindler TH, Montecucco F. Septic Cardiomyopathy: From Pathophysiology to the Clinical Setting. Cells. 2022; 11: 2833.

[3] Hollenberg SM, Singer M. Pathophysiology of sepsis-induced cardiomyopathy. Nature Reviews. Cardiology. 2021; 18: 424–434.

[4] Wang L, Ma XD, He HW, Su LX, Guo YH, Shan GL, *et al*. Analysis of factors influencing 3-and 6-h compliance with the surviving sepsis campaign guidelines based on medical-quality intensive care unit data from China. Chinese Medical Journal. 2021; 134: 1747–1749.

[5] Kreuzer M, Butovas S, García PS, Schneider G, Schwarz C, Rudolph U, *et al*. Propofol Affects Cortico-Hippocampal Interactions via β3 Subunit-Containing $GABA_A$ Receptors. International Journal of Molecular Sciences. 2020; 21: 5844.

[6] Lu M, Liu J, Wu X, Zhang Z. Ciprofol: A Novel Alternative to Propofol in Clinical Intravenous Anesthesia? BioMed Research International. 2023; 2023: 7443226.

[7] Wang C, Zhu L, Yuan W, Sun L, Xia Z, Zhang Z, *et al*. Diabetes aggravates myocardial ischaemia reperfusion injury via activating Nox2-related programmed cell death in an AMPK-dependent manner. Journal of Cellular and Molecular Medicine. 2020; 24: 6670–6679.

[8] Zhu Q, Li H, Xie X, Chen X, Kosuru R, Li S, *et al*. Adiponectin Facilitates Postconditioning Cardioprotection through Both AMPK-Dependent Nuclear and AMPK-Independent Mitochondrial STAT3 Activation. Oxidative Medicine and Cellular Longevity. 2020; 2020: 4253457.

[9] Xu Y, Pan S, Jiang W, Xue F, Zhu X. Effects of propofol on the development of cancer in humans. Cell Proliferation. 2020; 53: e12867.

[10] Guerrero Orriach JL, Raigon Ponferrada A, Malo Manso A, Herrera Imbroda B, Escalona Belmonte JJ, Ramirez Aliaga M, *et al*. Anesthesia in Combination with Propofol Increases Disease-Free Survival in Bladder Cancer Patients Who Undergo Radical Tumor Cystectomy as Compared to Inhalational Anesthetics and Opiate-Based Analgesia. Oncology. 2020; 98: 161–167.

[11] Lai HC, Lee MS, Lin C, Lin KT, Huang YH, Wong CS, *et al*. Propofol-based total intravenous anaesthesia is associated with better survival than desflurane anaesthesia in hepatectomy for hepatocellular carcinoma: a retrospective cohort study. British Journal of Anaesthesia. 2019; 123: 151–160.

[12] Cata JP, Forget P. Paravertebral block with propofol anaesthesia does not improve survival compared with sevoflurane anaesthesia for breast cancer surgery: independent discussion of a randomised controlled trial. British Journal of Anaesthesia. 2020; 124: 19–24.

[13] Han RH, Huang HM, Han H, Chen H, Zeng F, Xie X, *et al*. Propofol postconditioning ameliorates hypoxia/reoxygenation induced H9c2 cell apoptosis and autophagy via upregulating forkhead transcription factors under hyperglycemia. Military Medical Research. 2021; 8: 58.

[14] Du J, Zhou Y. Propofol reduces lipopolysaccharide induced cardiomyocyte injury in sepsis by activating SIRT1 mediated autophagy. Experimental and Therapeutic Medicine. 2023; 25: 187.

[15] Li Y, Guo T, Yang Z, Zhang R, Wang Z, Li Y. Effect of propofol versus midazolam on short-term outcomes in patients with sepsis-associated acute kidney injury. Frontiers in Medicine. 2024; 11: 1415425.

[16] Qi Z, Wang R, Liao R, Xue S, Wang Y. Neferine Ameliorates Sepsis-Induced Myocardial Dysfunction Through Anti-Apoptotic and Antioxidative Effects by Regulating the PI3K/AKT/mTOR Signaling Pathway. Frontiers in Pharmacology. 2021; 12: 706251.

[17] Gao G, Chen W, Yan M, Liu J, Luo H, Wang C, *et al*. Rapamycin regulates the balance between cardiomyocyte apoptosis and autophagy in chronic heart failure by inhibiting mTOR signaling. International Journal of Molecular Medicine. 2020; 45: 195–209.

[18] Pfalzgraff A, Weindl G. Intracellular Lipopolysaccharide Sensing as a Potential Therapeutic Target for Sepsis. Trends in Pharmacological Sciences. 2019; 40: 187–197.

[19] Rudiger A, Singer M. Mechanisms of sepsis-induced cardiac dysfunction. Critical Care Medicine. 2007; 35: 1599–1608.

[20] Im Y, Kang D, Ko RE, Lee YJ, Lim SY, Park S, *et al*. Time-to-antibiotics and clinical outcomes in patients with sepsis and septic shock: a prospective nationwide multicenter cohort study. Critical Care. 2022; 26: 19.

[21] Hunter JD, Doddi M. Sepsis and the heart. British Journal of Anaesthesia. 2010; 104: 3–11.

[22] Han X, Chen D, Liufu N, Ji F, Zeng Q, Yao W, *et al*. MG53 Protects against Sepsis-Induced Myocardial Dysfunction by Upregulating Peroxisome Proliferator-Activated Receptor-α. Oxidative Medicine and Cellular Longevity. 2020; 2020: 7413693.

[23] Sepúlveda M, Burgos JI, Ciocci Pardo A, González Arbelaez L, Mosca S, Vila Petroff M. CaMKII-dependent ryanodine receptor phosphorylation mediates sepsis-induced cardiomyocyte apoptosis. Journal of Cellular and Molecular Medicine. 2020; 24: 9627–9637.

[24] He Y, Wang S, Sun H, Li Y, Feng J. Naringenin ameliorates myocardial injury in STZ-induced diabetic mice by reducing oxidative stress, inflammation and apoptosis *via* regulating the Nrf2 and NF-κB signaling pathways. Frontiers in Cardiovascular Medicine. 2022; 9: 946766.

[25] Tang J, Hu JJ, Lu CH, Liang JN, Xiao JF, Liu YT, *et al*. Propofol inhibits lipopolysaccharide-induced tumor necrosis factor-alpha expression and myocardial depression through decreasing the generation of superoxide anion in cardiomyocytes. Oxidative Medicine and Cellular Longevity. 2014; 2014: 157376.

[26] Ullah E, El-Menyar A, Kunji K, Elsousy R, Mokhtar HRB, Ahmad E, *et al*. Untargeted Metabolomics Profiling Reveals Perturbations in Arginine-NO Metabolism in Middle Eastern Patients with Coronary Heart Disease. Metabolites. 2022; 12: 517.

[27] Wang AJ, Tang Y, Zhang J, Wang BJ, Xiao M, Lu G, *et al*. Cardiac SIRT1 ameliorates doxorubicin-induced cardiotoxicity by targeting sestrin 2. Redox Biology. 2022; 52: 102310.

[28] Zhang Y, Yang N, Huang X, Zhu Y, Gao S, Liu Z, *et al*. Melatonin Engineered Adipose-Derived Biomimetic Nanovesicles Regulate Mitochondrial Functions and Promote Myocardial Repair in Myocardial Infarction. Frontiers in Cardiovascular Medicine. 2022; 9: 789203.

[29] He Q, Pu J, Yuan A, Yao T, Ying X, Zhao Y, *et al*. Liver X receptor agonist treatment attenuates cardiac dysfunction in type 2 diabetic db/db mice. Cardiovascular Diabetology. 2014; 13: 149.

[30] Ge M, Chen H, Zhu Q, Cai J, Chen C, Yuan D, *et al*. Propofol post-conditioning alleviates hepatic ischaemia reperfusion injury via BRG1-mediated Nrf2/HO-1 transcriptional activation in human and mice. Journal of Cellular and Molecular Medicine. 2017; 21: 3693–3704.

[31] Zhang Y, Tan X, Cao Y, An X, Chen J, Yang L. Punicalagin Protects against Diabetic Liver Injury by Upregulating Mitophagy and Antioxidant Enzyme Activities. Nutrients. 2022; 14: 2782.